RESEARCH ON LASER-ACCELERATED PROTON GENERATION AT KAERI

SEONG HEE PARK*, KITAE LEE, YOUNG HO CHA, YOUNG UK JEONG,
SUNG HOON BAIK and BYUNG DUK YOO
Korea Atomic Energy Research Institute
150 Dukjin-dong, Yuseong-gu, Daejeon, Korea, 305-353
*Corresponding author. E-mail : shpark@kaeri.re.kr

Received August 17, 2004
Accepted for Publication April 27, 2005

A prototype of a relativistic proton generation system, based on laser-induced plasma interaction, has been designed and fabricated. The system is composed of three major parts: a fs TW laser; a target chamber, including targets and controls; and a diagnostic system for charged particles and lasers. An Offner-type pulse stretcher for chirped pulse amplification (CPA) and eight pass pre-amplifier are installed. The main amplifier will be integrated with a new pumping laser. The design values of the laser at the first stage are 1 TW in power and 50 fs in pulse duration. We expect to generate protons with their maximum energy of approximately 3 MeV and the flux of at least 10^6 per pulse using a 10 μm Al target. A prototype target chamber with eight 8-inch flanges, including target mounts, has been designed and fabricated. For laser diagnostics, an adaptive optics based on the Shack-Hartmann type, beam monitoring, and alignment system are all under development. For a charged particle, CR-39 detectors, a Thomson parabola spectrometer, and Si charged-particle detectors will be used for the density profile and energy spectrum. In this paper, we present the preliminary design for laser-induced proton generation. We also present plans for future work, as well as theoretical simulations.

KEYWORDS : Laser-plasma Interaction, Proton Generation, X-rays, Femtosecond Lasers, Chirped Pulse Amplification

1. INTRODUCTION

Ultra-intense laser systems based on solid state lasers have been developed and utilized for decades, mainly for laser-produced plasma and fusion research. In an early stage of laser-induced plasma research, a Nd:glass laser could produce a laser intensity of up to about 10^{16} W/cm^2; however, it had a low repetition rate, generally a few shots per hour, mainly due to the cooling of its large amplifiers with their high thermal loads. In the mid 1980's, the development of chirped pulse amplification (CPA) technology [1] dramatically changed the concepts of ultra-intense lasers. The basic idea is to stretch an ultrashort laser pulse before amplification, thereby lengthening its pulse duration and lowering its peak power, and to compress it after sufficient amplification, thereby generating a very high-powered laser pulse with an ultrashort duration. This scheme enabled researchers to avoid damage of optical components by operating the laser system below the damage threshold and to achieve very high power with relatively small laser energy, thereby tolerating the operation of a high repetition rate. After compression, the peak laser power of this system can reach terawatts or even petawatts, producing focused intensities of up to 10^{22} W/cm^2 [2].

CPA technology and broadband gain media now make it possible to generate ultrashort pulses and ultra high peak power at reasonable cost and scale. The cost reduction and table-top scale have had a great effect on the growth of research communities related to ultra-intense lasers, as well as on their applications. For the developed femto-second TW or PW lasers, a rapid expansion of applications has occurred in various fields: ultrafast science, laser acceleration, laser-driven particle or X-ray generation, laser fusion, and so on. In addition, the measurement, control, and/or synchronization techniques in femto-second scales have become critical design issues for lasers, X-rays, and charged particle beams. A large amount of research and development related to fs lasers has opened up new fields in physics.

Various, worldwide studies of laser-driven charged-particle generation have been performed for the last few decades. In the beginning, accelerated ions, like proton, copper, carbon, and etc, were detected as an unwanted by-product in laser fusion experiments and were categorized as potential problems. Gitomer et al. [3] began to investigate the relationship between ion energy and hot-electron temperature and suggested several models to explain the

physics of ion acceleration through experimental and theoretical analysis. In the 1990s, several laboratories [4-8] successfully generated (or accelerated) laser-induced MeV protons using an fs TW laser and suggested many applications using them. For medical applications, the miniaturization of a proton source and the reduction of radiation hazards have emerged as a great merit. More studies are still needed to understand the physics of ion-acceleration mechanism and to control the conditions for the desired ions of each application. In addition to proton generation, laser-plasma interactions make it possible to produce other useful particles and high-energy photons, such as neutrons, heavy ions, X-rays, and gamma rays, and so enormous possibilities exist for further application of the technology. The Korea Atomic Energy Research Institute (KAERI) recently proposed a project involving laser-driven charged-particle generation as a spin-off project based on R&D laser technologies.

2. ESSENTIALS OF HIGH-ENERGY PROTON GENERATION

Laser-induced radiation, in such forms as high-energy X-rays and ions, is caused by the generation of fast electrons resulting from laser-plasma interactions. In all high-energy ion-generation experiments, fast electrons, with greater energy than ions, have been observed and described as a primary effect. Though a number of mechanisms have been proposed to explain their appearance, the precise origin of the energetic protons has not yet been verified and has maintained significant scientific interest.

According to the interpretation of the Lawrence Livermore National Laboratory (LLNL) [9], free electrons in plasma accelerate through the target via a $\mathbf{v} \times \mathbf{B}$ force and then form the Debye sheath. This electron sheath reflects consecutive electrons from both sides of sheath. When it arrives at the backside of the target, an increased electron density creates an electric field for the proton (or ion) acceleration. Mackinnon et al. [10] observed a strong dependency of the proton energy yield on the target thickness and explained this dependency using a recirculation model of electrons combined with the previous model.

In general, the maximum energy of protons can be estimated by using the scaling relation given by the equation [4, 12]

$$E_{p,Max} = (const.) \times (I\lambda^2)^{0.3\sim0.5}, \quad (1)$$

where I is the laser intensity and λ is the laser wavelength, $E_{p,Max}$ is the maximum proton energy in MeV. Typically, $I\lambda^2 \sim 10^{14}$ - 10^{19} W/cm^2. The exponent number varies slightly, depending on the experimental conditions. The yield of protons increases as the maximum energy of protons is increased. Currently, the maximum energy reported has been about 58 MeV, yielding 30 trillion protons, at Livermore's NOVA Petawatt laser [13]. Several other groups have also reported successful generations of tens of MeV protons [14-16].

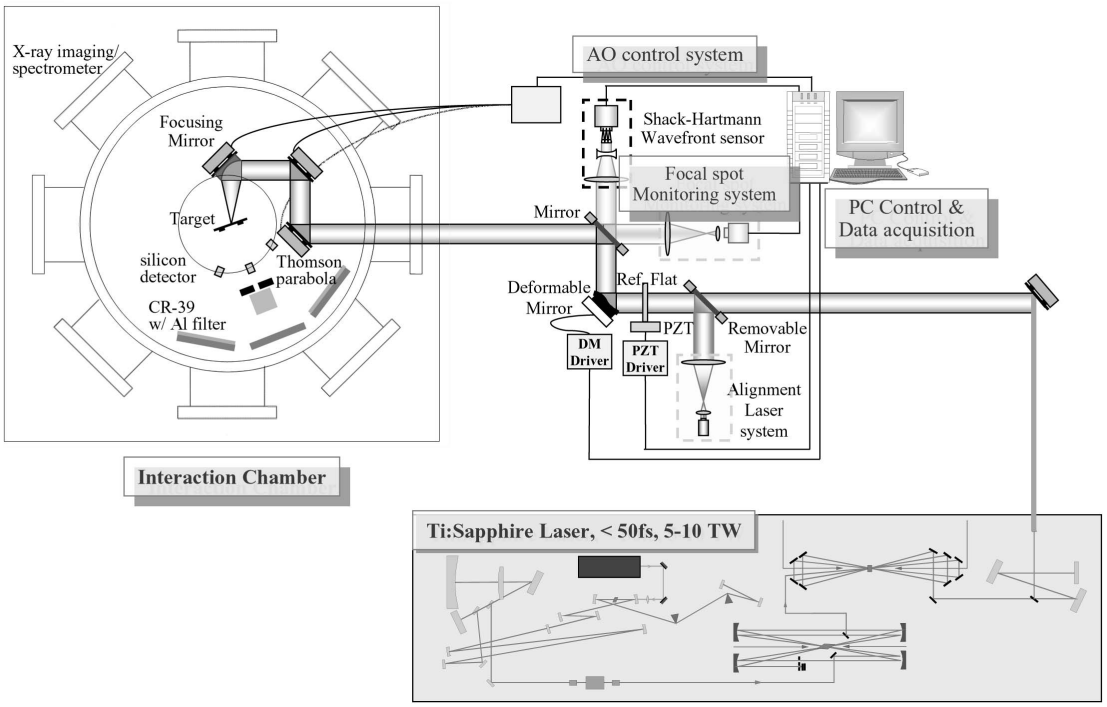

Fig. 1.Overall Layout for the Experimental Set-up

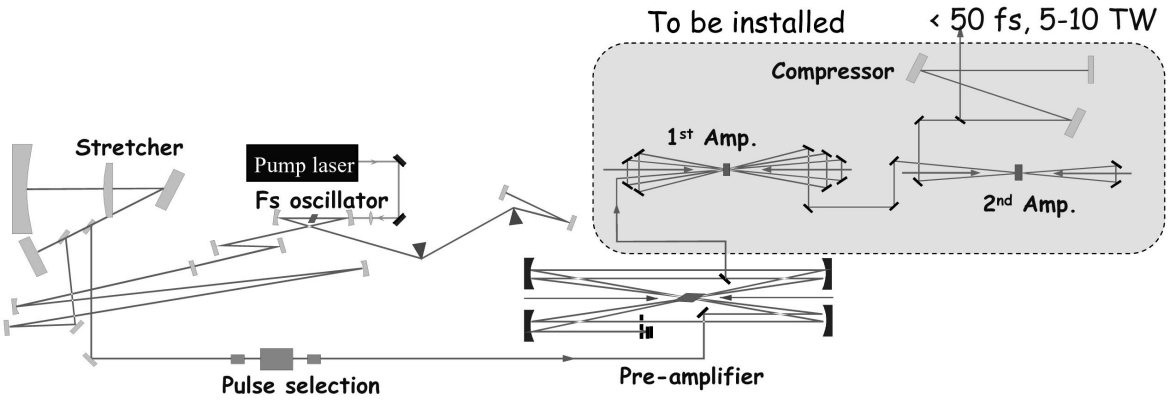

Fig. 2. Schematic of a Fs High-power Laser System at KAERI

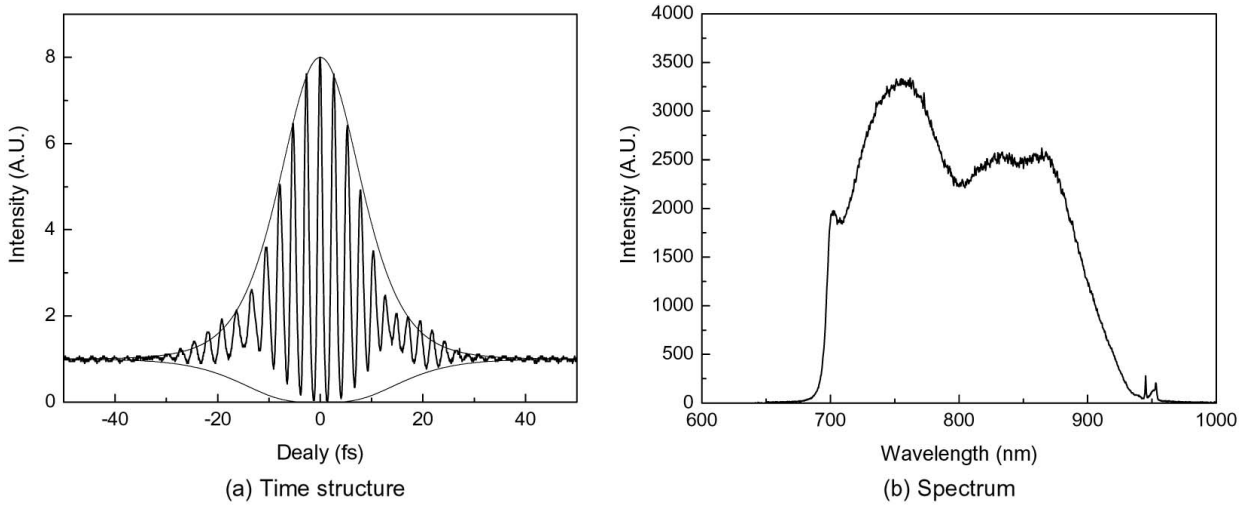

Fig. 3. Time Structure and Spectrum of the Fs Ti:sapphire Laser at the Oscillator

3. PRELIMINARY SET-UP FOR PROTON GENERATION EXPERIMENTS

There are three major parts to the considered proton generation system: an fs TW laser system, a target chamber, and a detection and diagnostic system. An overall schematic is shown in Figure 1. An fs Ti:sapphire laser system is under development; it is composed of an oscillator, a stretcher, a pre-amplifier, a two-staged main amplifier, and a compressor. A deformable mirror and an off-axis parabolic mirror are used to correct the laser wavefront after the compression and the focusing of the laser beam at the target, respectively. The diagnostic system, alignment system, and beam profile monitoring system are all under development.

3.1 An fs High-power Laser System

As illustrated in Figure 2, the laser system uses a Kerr-lens mode-locked Ti:sapphire laser oscillator [17], pumped by a frequency-doubled Nd:YVO_4 laser (Spectra-Physics, Millennia Vs). The oscillator operates at a repetition rate of 100 MHz, and the average output power is 350 mW at a 3 W pumping power. As illustrated in Figure 3, at the oscillator, the output spectrum is centered at about 800 nm with a bandwidth of more than 150 nm, and the pulse duration is 15 fs, as measured by an autocorrelator. The pulses from the oscillator are stretched to 200 ps by an Offner-type pulse stretcher and are selected by a Pockels cell. A selected pulse is amplified to 4 mJ by an 8-pass pre-amplifier pumped by a Q-switched frequency-doubled Nd:YAG laser operating at 10 Hz. Currently, we are preparing a two-staged main amplification system, 5-pass and 2-pass amplifiers, and a pulse compressor, with which to boost the pulse energy to above 300 mJ and to generate sub-30-fs pulses with a peak power of more than 5 TW.

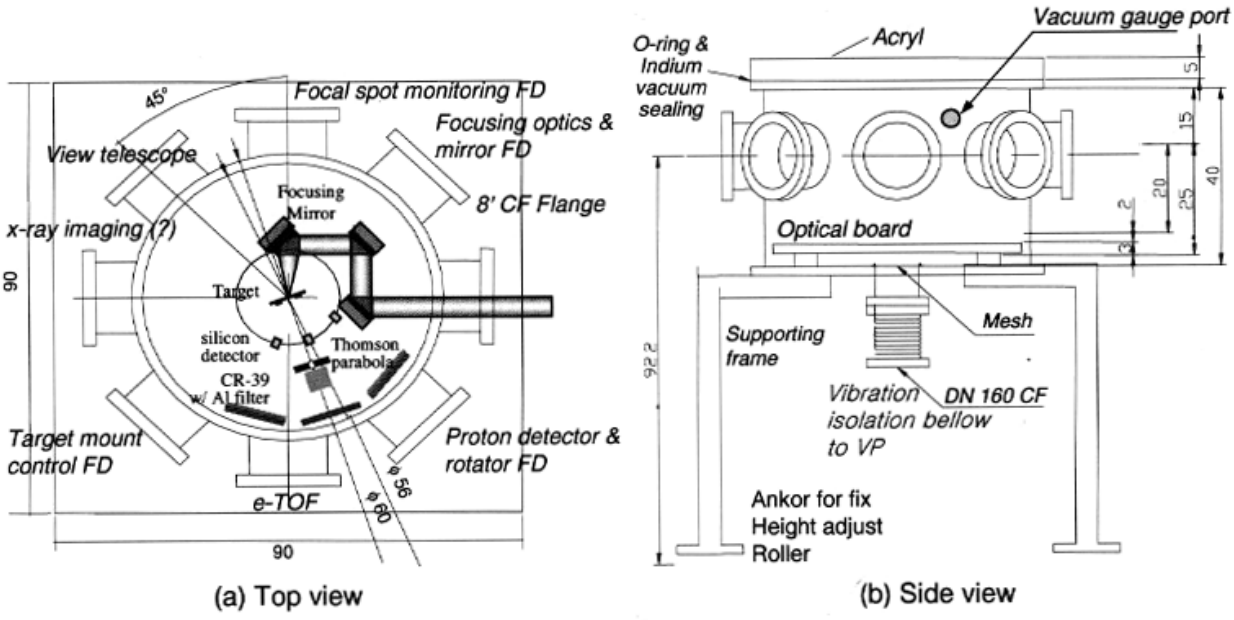

Fig. 4. Schematics of the Target Chamber

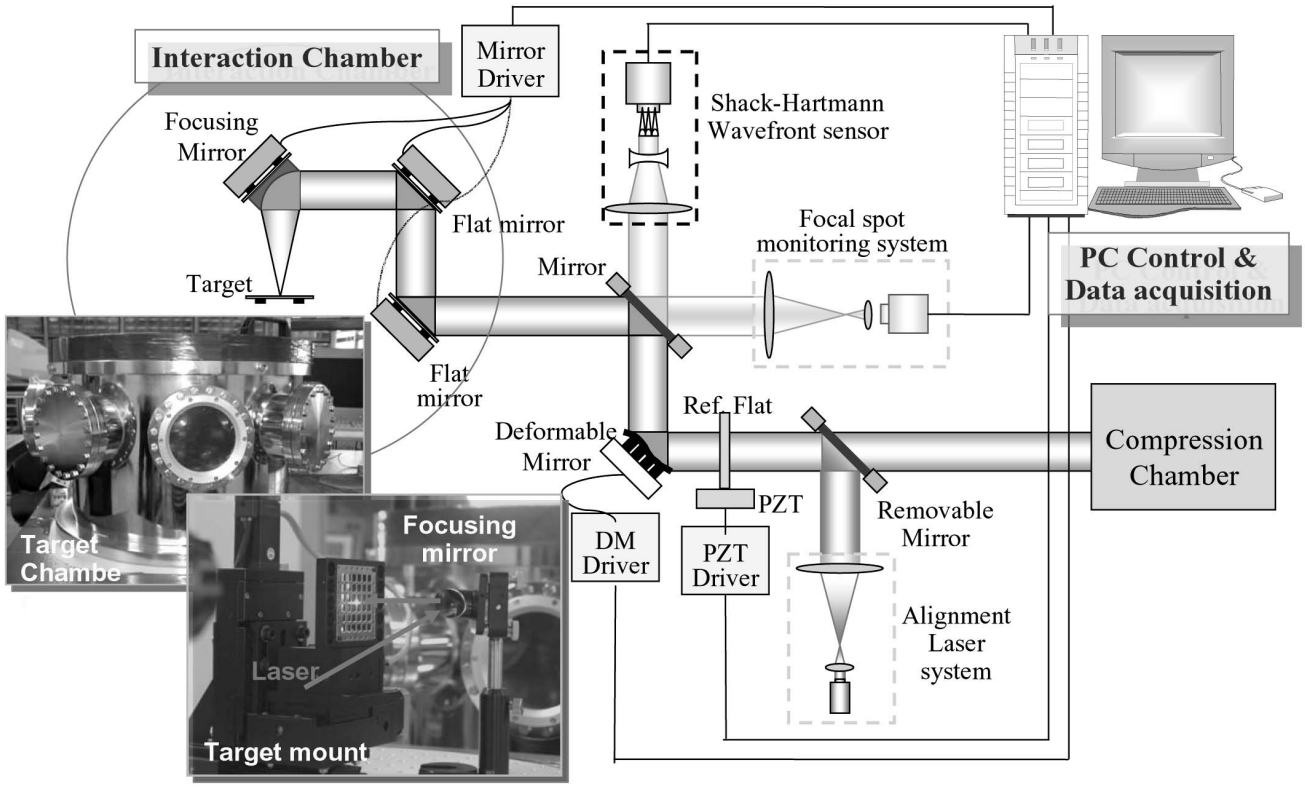

Fig. 5. Layout of Beam Delivery and Laser Diagnostic System

3.2 A Target Chamber

A prototype target chamber was designed and fabricated, as shown in Figure 4. The chamber is cylindrically shaped, with a diameter and height of 60 cm and 40 cm, respectively. It is composed of eight 8-inch flanges used to transport the incident laser, connectors for control signals and for remote-control system power supplies, a diagnostic system, and detection systems. The chamber was designed to have flexible fittings for various possible applications.

The laser beam is delivered to the target by one or two flat mirrors inside the chamber and an off-axis parabola mirror for final focusing. The flat mirrors facilitate the alignment of the laser beam and protect the window against damage from debris. The target mount is designed to use either a solid target or a film target. For film targets, a reel-type target mount is used for targets of a few micrometers in thickness, while a wheel type target mount is used for sub-micrometer-thick targets. For a preliminary test, a meshed target mount with 6×6 openings will be used with 2-D translational stages.

A turbo pumping system under a vacuum chamber was installed to keep the vacuum below 10^{-7} torr, and a bellow was installed between the pumping system and the chamber to isolate the target chamber from mechanical vibration. The material of the prototype chamber is stainless steel, and the local shielding materiala and their thickness to be installed inside can vary, depending on the kind of particles and their energy.

3.3 Beam Diagnostic Systems

An adaptive optics system using the Shack-Hartmann wavefront sensor was tested to determine its compensation efficiency for an arbitrary wavefront distortion [18]. It was found that an arbitrary distorted wavefront from a He-Ne laser can be improved from 5λ to $\lambda/2$ at a wavelength of 632.8 nm and, consequently, the laser intensity on the target may be increased by at least a factor of four. The intensity of incident laser on targets is important factor in characterizing the generated protons, due to their strong dependency on flux and energy. For beam diagnostics, a real-time measurement system of laser-beam profile on the target is utilized by means of telescope optics and a CCD camera. A laser footprint at the front surface of a movable screen located at the center of the chamber (or at the target mount) will be measured directly at low intensity for the absolute reference, and the image reflected from the target will be monitored and calibrated with the reference. The position of the focal point can be located on the target with an accuracy of a few μm. A He-Ne laser is used for the pre-alignment of the incident laser beam, as shown in Figure 5.

For measurements of charged particles, CR-39 track detectors, silicon detectors, and a Thomson parabola detector will be used for the measurement of the energy spectrum. The silicon detection system (Ortec) can be used to measure the angular energy distribution. This system includes silicon detectors, amplifiers, a multi-channel buffer, and a data acquisition system, and it enables analysis of protons with energies of 0.1- 6 MeV with an accuracy of 12 keV of α-particles. The range and the resolution of energy are limited by the specifications of the silicon detectors. CR-39 track detectors will be used as a stack of several films, consisting of Radiochromic films (RCFs) as density profiler and/or metal/mylar film as a filter.

The Thomson parabola spectrometer is a prototype designed for proton energies below 10 MeV, and its typical geometry is shown in Figure 6. The gap, d, and the length, L, of a magnet are 3 mm and 4.5 cm, respectively. The CR-39 plate is located 15 cm away from the magnet and two pinholes are used as a collimator. The expected trajectories at the screen for different charged particles are calculated with a given magnetic field and an electric field

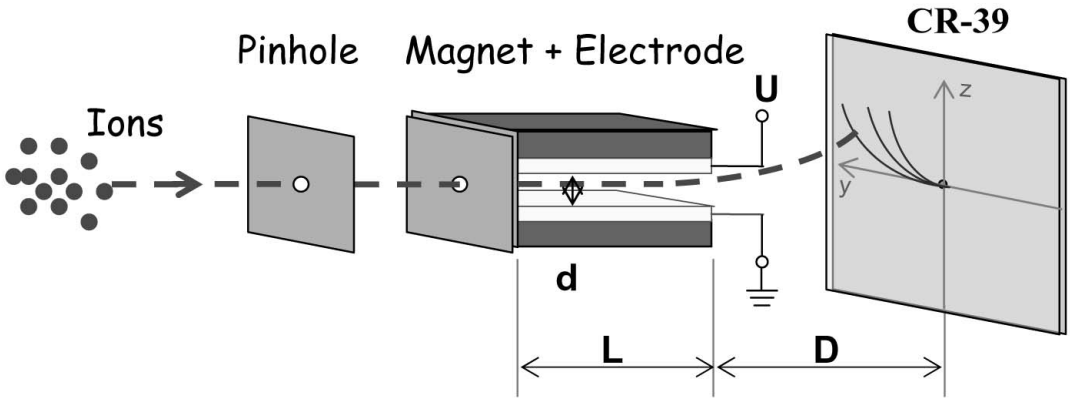

Fig. 6. Geometry of Thomson Parabola Spectroscope

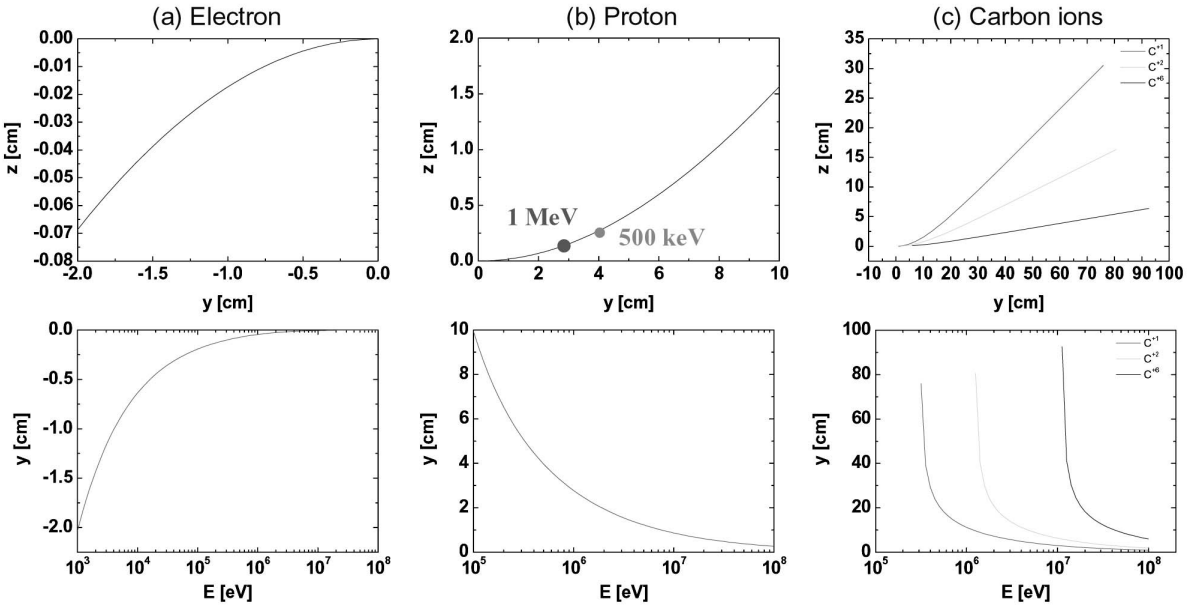

Fig. 7. Trajectories of Charged Particles Depending on their Energy and Mass

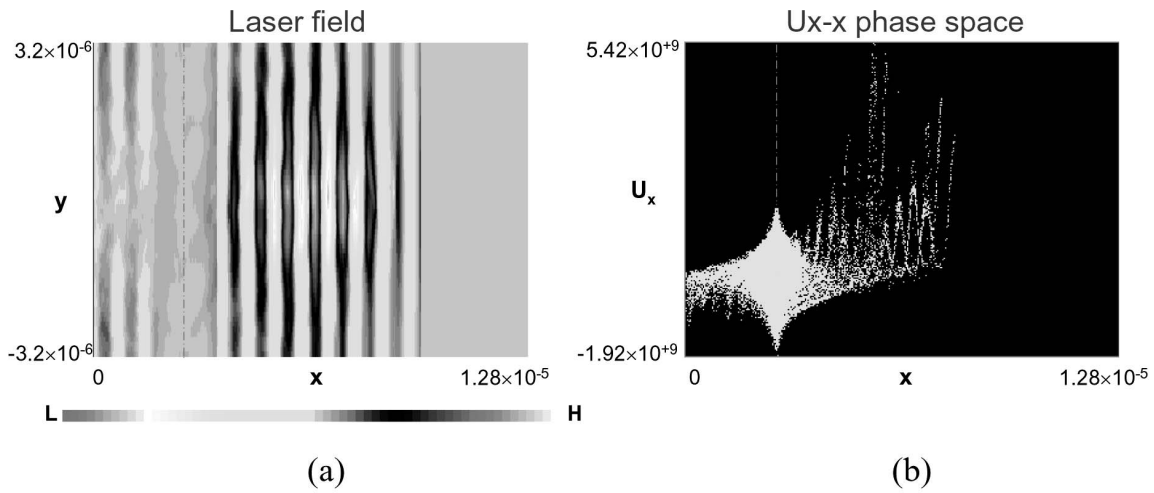

Fig. 8. Simulation Results of Laser Field and Velocity of Particles Along the Propagation Direction x
(Intensity of a laser pulse on the target: 4×10^{19} W/cm^2)

of 5.1 kG and -1 kV, respectively, as shown in Figure 7.

4. SIMULATIONS

The interaction of an intense laser pulse with plasmas involves complicated and nonlinear physical processes, such as nonlinear laser propagation through the overdense plasma and various plasma dynamics, including particle accelerations and plasma wave generations. A particle simulation is essential to adequately describe such highly nonlinear and kinetic physical phenomena, both for an analysis of the experimental results and for an understanding of the underlying physical mechanism.

Simulation codes and a PC cluster system are under development. The PC cluster, called LAMP (LAser Matter interaction Physics), is composed of a master and four nodes, using five 2.8 GHz Intel Pentium IVs, a 1 Gigabyte

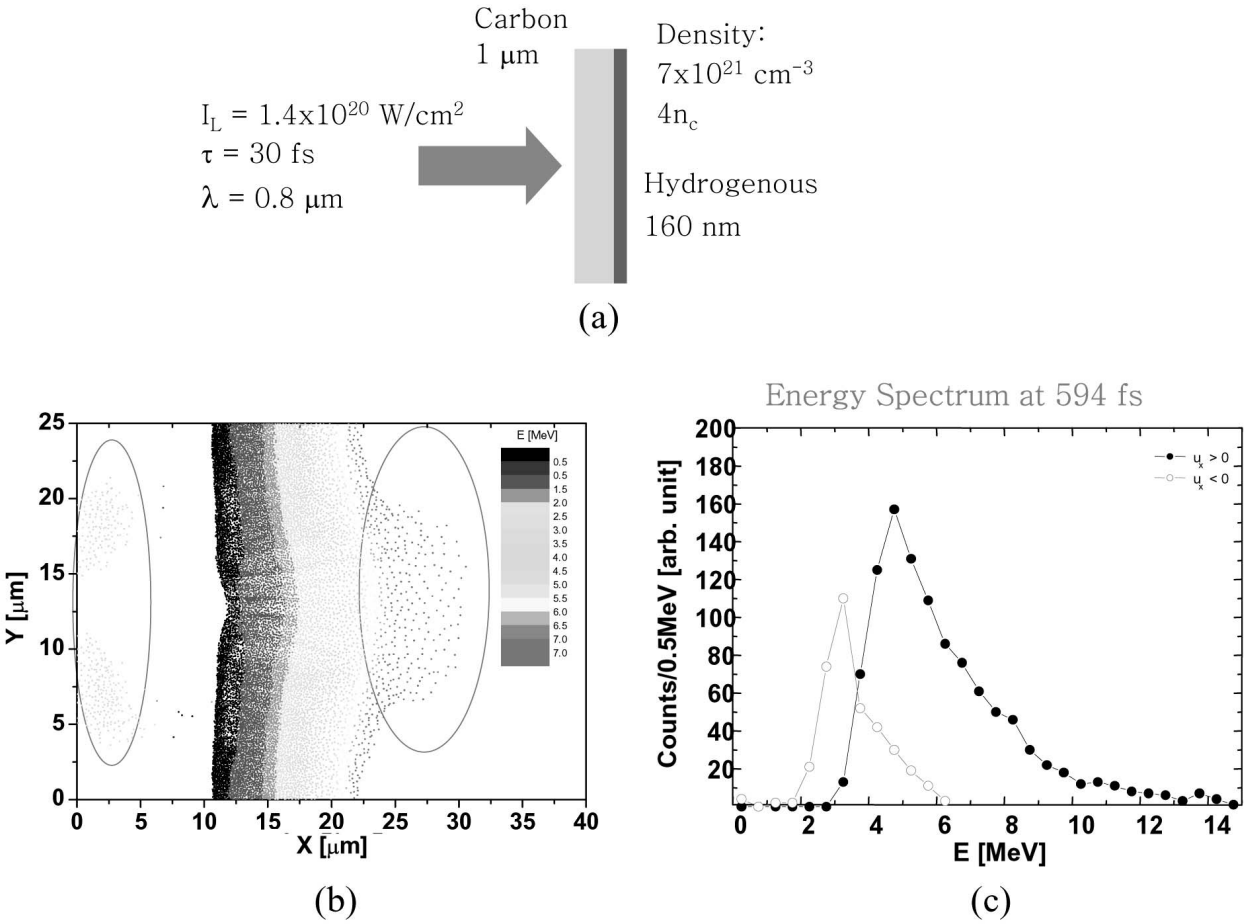

Fig. 9. Simulation Results of Proton Generation : (a) Initial Condition; (b) Spatial Distribution at 584 fs After; (c) Energy Spectrum of Generated Protons (Intensity of a laser pulse on the target: 1.4×10^{20} W/cm^2; Target: 1 mm Carbon)

Lan. For the operating system, Linux Red Hat 8.0. is used and, for the simulation code, X window Object Oriented Particle-In-Cell (XOOPIC), as developed by the plasma theory group, University of Berkeley (http://ptsg.eecs.berkeley.edu/), is used. It was adopted with consideration toward its computing efficiency and future extension.

To test the cluster system, a preliminary calculation was performed by irradiating a laser pulse of 30 fs at 800 nm with an intensity of 4×10^{19} W/cm^2 on a 50 nm thick Ti target. The initial density of the target is given to 10 times the critical plasma density, which is close to the solid density. Figures 8 (a) and 8 (b) show the propagation of the intense laser pulse and the dynamics of electrons in the phase space, respectively. The result shows that the intense laser pulse transparently propagates through the overdense plasma if the thickness of the plasma is much shorter than the plasma skin depth, which is around 200 nm in this case. A detailed analysis of the dynamics of an ultra-thin plasma can be performed in future experiments, since such thin targets have recently become commercially available.

As shown in Fig. 9, a virtual target with a double-layered structure, 1 μm of carbon and 160 nm of a proton-enriched layer, is used for proton generation. A laser with pulse duration of 30 fs at 800 nm is normally incident on the target, resulting in an intensity of 1.4×10^{20} W/cm^2. The protons accelerated in the forward direction have a higher peak energy compared to those in the backward direction, and both spectra are peaked with a few 10% of energy spread. Further calculations are required both for an analysis of the experimental results and for an understanding of the underlying physical mechanism

5. SUMMARY

An experimental set-up for relativistic charged particle generation is near completion. We expect that the first demonstration with the KAERI laser system will be performed in the fall of 2005. Using a TW laser focused

to a 10 μm spot size, we expect that the energy and flux of the proton generated with Al targets will be less than 3 MeV and about 10^6 particles per pulse, respectively. We expect to obtain a laser power of up to 5 TW with a newly purchased pumping laser and to generate energetic protons of higher than 3 MeV. We plan to use several types of targets with different thicknesses, down to the sub-μm thickness range. We also plan to upgrade our laser system to 10 TW in the near future and to collaborate with other laboratories in Korea and Japan.

REFERENCES

[1] D. Strickland, G. Mourou, "Compression of Amplified Chirped Optical Pulses," Opt. Comm. 56, 219 (1985)

[2] Reference in http://wwwapr.apr.jaeri.go.jp/jaeri/e/ICUIL/DBW-Laser01u.pdf; S.-W. Bahk, P. Rousseau, T. A. Planchon, V. Chvykov, G. Kalintchenko, A. Maksimchuk, G. A. Mourou, V. Yanovsky, "Generation and characterization of the highest laser intensities (1022 W/cm2)", Optics Letters 29, Issue 24, 2837-2839 (2004);

[3] S.J. Gitomer, R.D. Jones, F. Bergay, A.W. Ehler, J.F. Kephart, R. Kristal, "Fast ions and hot electrons in the laser–plasma interaction," Phys. Fluids 29, 2679 (1986).

[4] F.N. Beg, A.R. Bell, A.E. Dangor, C.N. Danson, A.P.Fews, M.E. Glinsky, B.A. Hammel, P. Lee, P.A. Norreys, M. Tatarakis, "A study of picosecond laser–solid interactions up to 10^{19} W/cm^2," Phys. Plasmas 4, 447 (1997).

[5] E.L. Clark, K. Krushelnick, J.R. Davies, M. Zepf, M. Tatarakis, F.N. Beg, A. Machacek, P.A. Norreys, M.I.K. Santala, I. Watts, A.E. Dangor, "Measurements of energetic proton transport through magnetized plasma from intense laser interactions with solids," Phys. Rev. Lett. 84, 670 (2000).

[6] A. Maksimchuk, S. Gu, K. Flippo, D. Umstadter and V. Yu. Bychenkov, "Forward Ion Acceleration in Thin Films Driven by a High-Intensity Laser," Phys. Rev. Lett. **84**, 4108 (2000).

[7] R.A. Snavely, M.H. Key, S.P. Hatchett, T.E. Cowan, M. Roth, T.W. Phillips, M.A. Stoyer, E.A. Henry, T.C. Sangster, M.S. Singh, S.C. Wilks, A. MacKinnon, A. Offenberger, D.M. Pennington, K. Yasuike, A.B. Langdon, B.F. Lasinski, J. Johnson, M.D. Perry, E.M. Campbell, "Intense high-energy proton beams from petawatt-laser irradiation of solids," Phys. Rev. Lett. **85**, 2945 (2000).

[8] M. Zepf, E. L. Clark, K. Krushelnick, F. N. Beg, A. E. Dangor, M. I. K. Santala, M. Tatarakis, I. F. Watts, P. A. Norreys, R. Clarke, J. R. Davies, M. Sinclair, R. Edwards, T. Goldsack, I. Spencer, and K. W. D. Ledingham, "Fast particle generation and energy transport in laser-solid interactions," Physics of Plasmas 8, 2323 (2001).

[9] S. C. Wilks, A. B. Langdon, T. E. Cowan, M. Roth, M. Singh, S. Hatchett, M. H. Key, D. Pennington, A. MacKinnon, and R. A. Snavely "Energetic proton generation in ultra-intense laser–solid interactions", Phys. Plasmas **8**, 542 (2001); References therein.

[10] A. J. Mackinnon, Y. Sentoku, P. K. Patel, D. W. Price, S. Hatchett, M. H. Key, C. Andersen, R. Snavely, R. R. Freeman, "Enhancement of Proton Acceleration by Hot-Electron Recirculation in Thin Foils Irradiated by Ultraintense Laser Pulses," Phys. Rev. Lett. **88**, 215006 (2000).

[11] M. Allen, Y. Sentoku, P. Audebert, A. Blazevic, T. Cowan, J. Fuchs, J.C. Gauthier, M. Geissel, M. Hegelich, S. Karsch, E. Morse, P.K. Patel, M. Roth, "Proton spectra from ultraintense laser-plasma interaction with thin foils: Experiments, theory, and simulation," Physics of Plasma 10, 3283 (2003)

[12] E.L.Clark, K.Krushelnick, M.Zepf, F.N.Beg, A.Machacek, M.I.K.Santala, M.Tatarakis, I.Watts, P.A.Norreys, and A.E.Dangor, "Energetic heavy-ion and proton generation from ultraintense laser-plasma interactions with solids," Phys. Rev. Lett. 85, 1654 (2000)

[13] R. A. Snavely, M. H. Key, S. P. Hatchett, T. E. Cowan, M. Roth, T. W. Phillips, M. A. Stoyer, E. A. Henry, T. C. Sangster, M. S. Singh, S. C. Wilks, A. MacKinnon, A. Offenberger, D. M. Pennington, K. Yasuike, A. B. Langdon, B. F. Lasinski, J. Johnson, M. D. Perry, and E. M. Campbell, "Intense High-Energy Proton Beams from Petawatt-Laser Irradiation of Solids," Phys. Rev. Lett. 85, 2945-2948 (2000)

[14] M. Borghesi, A.J. Mackinnon, D.H. Campbell, D.G. Hicks, S. Kar, P.K. Patel, D. Price, L. Romagnani, A. Schiavi, and O. Willi, "Multi-MeV Proton Source Investigations in Ultraintense Laser-Foil Interactions", Phys. Rev. Lett. 92, 055003 (2004)

[15] T.E. Cowan, J. Fuchs, H. Ruhl, A. Kemp, P. Audebert, M. Roth, R. Stephens, I. Barton, A. Blazevic, E. Brambrink, J. Cobble, J. Fernadez, J.-C. Gauthier, M. Geissel, M. Hegelich, J. Kaae, S. Karsch, G.P. Le Sage, S. Letzring, M. Manclossi, S. Meyroneinc, A. Newkirk, H. Pepin, N. Renard-LeGalloudec, "Ultralow, Multi-MeV Proton Beams from a Laser Virtual-Cathode Plasma Accelerato", Phys. Rev. Lett. 92, 204801 (2004)

[16] M. Zepf, E. L. Clark, F. N. Beg, R.J. Clarke, A. E. Dangor, A. Gopal, K. Krushelnick, M. P. A. Norreys, M. Tatarakis, U. Wagner, M.S. Wei, "Proton Acceleration from High-Intensity Laser Interactions with Thin Foil Targets," Phys. Rev. Lett. 90, 064801 (2003).

[17] Yong Ho Cha, Kitae Lee, Jae Min Han, Yong Joo Rhee, "Sequence effect of optical elements in a femtosecond Ti:sapphire laser oscillator," JOSA B, Vol. 20, Issue 6, 1369-1373 (2003).

[18] S. H. Baik, S. K. Park, C. J. Kim, Y. S. Seo, Y. J. Kang, "New centroid detection algorithm for Shack-Hartmann wavefront sensor," *Proceedings of SPIE* Vol.4926, 251-260 (2003)